INTERNATIONAL SOCIETY FOR
SOIL MECHANICS AND
GEOTECHNICAL ENGINEERING

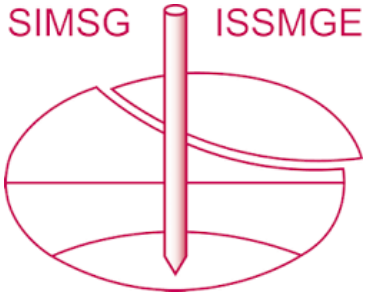

This paper was downloaded from the Online Library of the International Society for Soil Mechanics and Geotechnical Engineering (ISSMGE). The library is available here:

https://www.issmge.org/publications/online-library

This is an open-access database that archives thousands of papers published under the Auspices of the ISSMGE and maintained by the Innovation and Development Committee of ISSMGE.

The paper was published in the proceedings of the 10th International Conference on Physical Modelling in Geotechnics and was edited by Moonkyung Chung, Sung-Ryul Kim, Nam-Ryong Kim, Tae-Hyuk Kwon, Heon-Joon Park, Seong-Bae Jo and Jae-Hyun Kim. The conference was held in Daejeon, South Korea from September 19th to September 23rd 2022.

Physical Modelling in Geotechnics
© 2022 KOREAN GEOTECHNICAL SOCIETY (KGS), Seoul, Korea, ISBN 978-89-952197-7-5

Monitoring bending moment distributions in large-scale laterally loaded piles using fibre Bragg gratings and vibrating wire strain gauges

R.A. Murison, S.W. Jacobsz & T.S. da Silva Burke
Department of Civil Engineering, University of Pretoria, South Africa

T.A.V. Gaspar & A.S. Osman
Department of Engineering, Durham University, United Kingdom

ABSTRACT: Reinforced-concrete bored piles were installed in an expansive clay profile near Vredefort, South Africa. Each pile was instrumented with 6 vibrating wire strain gauges (VWSGs) and 20 fibre Bragg gratings (FBGs). Static and cyclic lateral loads were applied to the pile heads to simulate the cyclic nature of loading on wind turbine foundations. This study compares the bending moment distributions determined using the two types of strain gauge. The suitability of each for large-scale physical modelling and structural health monitoring has been evaluated. The fibre Bragg gratings delivered similar results to the vibrating wire gauges when measuring tensile strains, but underpredicted compressive strains. Due to closer spacing, the strain distributions determined from the Bragg gratings illustrated greater detail of localised strains where cracking had occurred on the tension side of the piles.

Keywords: strain instrumentation, large-scale modelling, structural health monitoring, pile foundations, swelling clay

1 INTRODUCTION

This study was conducted as part of the WindAfrica project, funded by the EPSRC (UK), investigating the behaviour of wind turbine piled foundations in unsaturated expansive clay. An overview of the project is given by Gaspar et al. (2022). The physical modelling used to investigate various aspects of the problem included both centrifuge testing and large-scale field tests. Results reported in this study are for lateral pile loading tests on the free-headed large-scale piles installed in a highly expansive clay profile near Vredefort, South Africa. Details of the site conditions and field installations are given by da Silva Burke et al. (2022) and descriptions of the swelling behaviour of the clay profile are given by Murison et al. (2022).

2 INSTRUMENTATION LAYOUT

Reinforced-concrete bored piles with 600 mm diameters were installed to a depth of 6 m. Each pile was instrumented with 20 fibre Bragg gratings (FBGs) and 6 vibrating wire strain gauges (VWSGs). The positioning of the strain gauges is illustrated schematically in Fig. 1. Lateral loads were applied to the pile head 500 mm above the natural ground level under load control using a hydraulic jack.

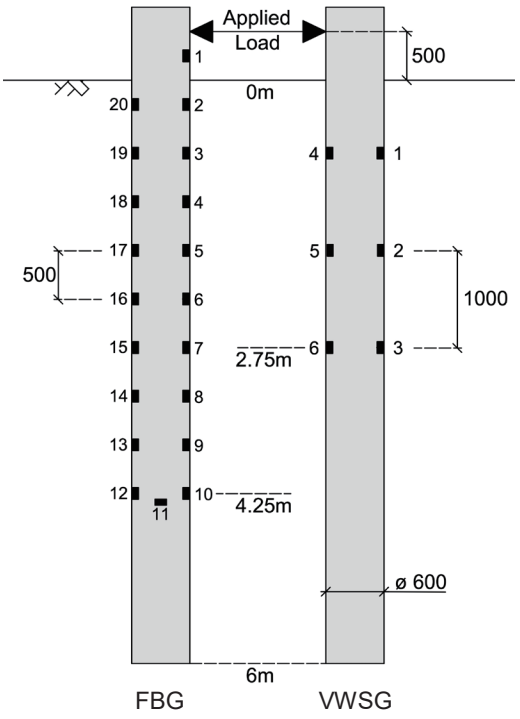

Fig. 1. Strain gauge spacing with depth.

3 STRAIN GAUGES

Geosense VWS-2100 vibrating wire strain gauges were embedded within the bored piles. Specifications are given in Table 1 (after Geosense, 2021). FBGS DTG-

© 2022 KOREAN GEOTECHNICAL SOCIETY (KGS), Seoul, Korea, ISBN 978-89-952197-7-5

LBL-1550 draw tower gratings were used for fibre optic sensing. The fibre Bragg grating arrays were housed within a 1.0 mm glass fibre reinforced plastic (GFRP) round profile and 0.5 mm HDPE casing. A wavelength configuration between 1512 nm and 1588 nm in 4 nm steps was utilised. Specifications are given in Table 1 (after FBGS, 2020). The gauges are depicted in Fig. 2, and installation details are shown in Fig. 3.

Table 1. Strain gauge specifications (after Geosense, 2021 and FBGS, 2020).

	VWSG	FBG
Gauge length (mm)	150	8
Strain range (με)	3000	25000 *
Temperature range (ºC)	–20 to 95	–40 to 120

* maximum tensile strain

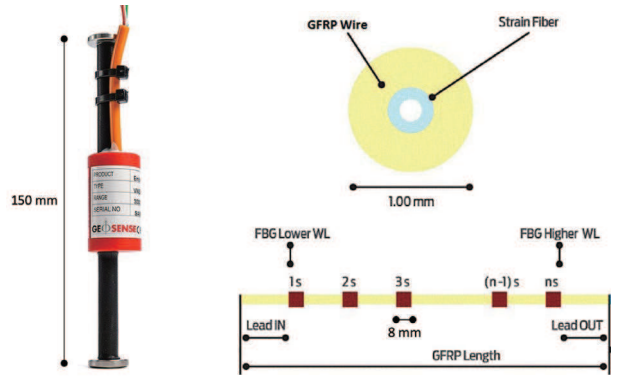

a) VWSG (Geosense, 2021) b) FBG (FBGS, 2021)

Fig. 2. Strain gauges used for monitoring.

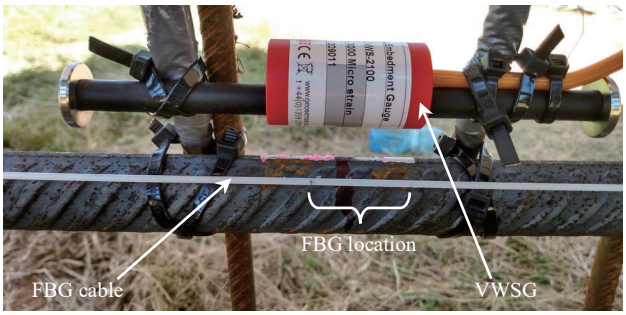

Fig. 3. Installation details of the VWSGs and FBGs.

The vibrating wire strain gauges report a change in resonant frequency of the strain gauge wire due to straining of the wire. The change in strain in the VWSGs ($\Delta\mathcal{E}_{VWSG}$) in units of microstrain ($\mu\varepsilon = 10^{-6}$ m/m) was calculated using Equation 1:

$$\Delta\mathcal{E}_{VWSG} = \left[\frac{f^2}{1000} - \frac{f_0^2}{1000}\right] \; G_F \; B_F \qquad (1)$$

where f is the given frequency reading in Hz, f_0 is the initial frequency reading, and the gauge factor (G_F) and batch factor (B_F) calibrated for the installed gauges were 3.718 and 0.958 respectively.

The fibre Bragg gratings report a change in the wavelength of backscattered light in the fibre optic cable due to straining of the cable. The wavelengths are monitored at discrete points with finite Bragg grating gauge lengths. The change in strain in the FBGs ($\Delta\mathcal{E}_{FBG}$), in microstrain, was calculated using Equation 2:

$$\Delta\mathcal{E}_{FBG} = 0.78\left[\frac{\lambda - \lambda_0}{\lambda_0}\right] \cdot 10^6 \qquad (2)$$

where λ is the given wavelength reading, λ_0 is the initial wavelength reading, and 0.78 is the strain-optic coefficient relating the relative change in wavelength of backscattered light to the strain in the fibre optic cable.

4 RESULTS

The bending moments at each depth were calculated by assuming a linear strain distribution between the tension and compression strain gauges. Composite section analysis principles per Eurocode 2 were utilised. (Mosley et al., 2012; BS EN1992:2004). The tensile capacity of the concrete was measured as 2.0 MPa; it was assumed that no tensile stress could be supported in concrete beyond this limit.

The bending moment and strain distributions of a pre-cracked laterally loaded free-headed pile are presented in Fig. 4. Shortcomings of each strain gauge layout could be observed in this test. Compressive strains were seemingly underpredicted by the FBGs. This possibly indicates that the pre-tensioning in the cable had relaxed prior to load application. In addition, inherent heterogeneities in concrete (such as coarse aggregate particles pressing against the gauge, or air pockets causing slippage/loss of bonding) could affect readings taken over the 8 mm FBG gauge length. The 150 mm VWSG gauge length would avoid these inconsistencies. However, the closer spacing of discrete strain measurements for the FBGs allowed distinct cracks to be better identified through spikes in the tensile strain distributions. Although the two tensile strain measurements were in good agreement at respective depths, the severity of the crack in the region of 1.25 m in Fig. 4 was not captured by the strain and bending moment distributions from the VWSGs. For structural health monitoring, where structural cracking and strain spikes are of interest, the fibre optic layout with greater achievable resolution (in terms of monitoring points with depth) would be more beneficial to an analyst.

Bending strains at various depths (z) determined using the VWSGs and FBGs at the outermost fibres of the concrete with monotonically increasing load are given in Fig. 5.

© 2022 KOREAN GEOTECHNICAL SOCIETY (KGS), Seoul, Korea, ISBN 978-89-952197-7-5

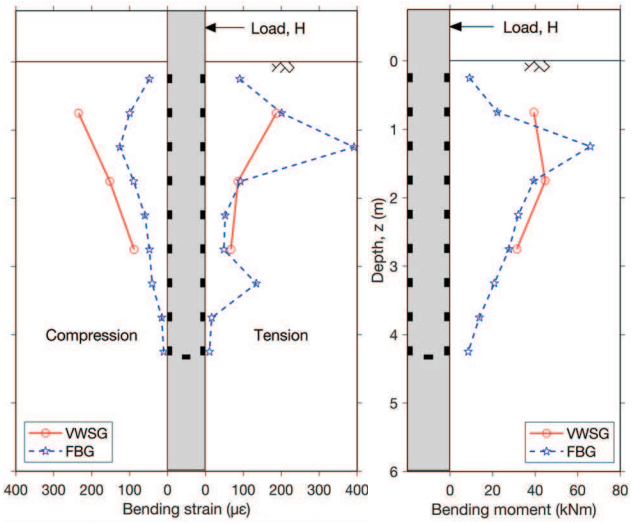

Fig. 4. Bending strain and moment of pre-cracked pile, H=120 kN.

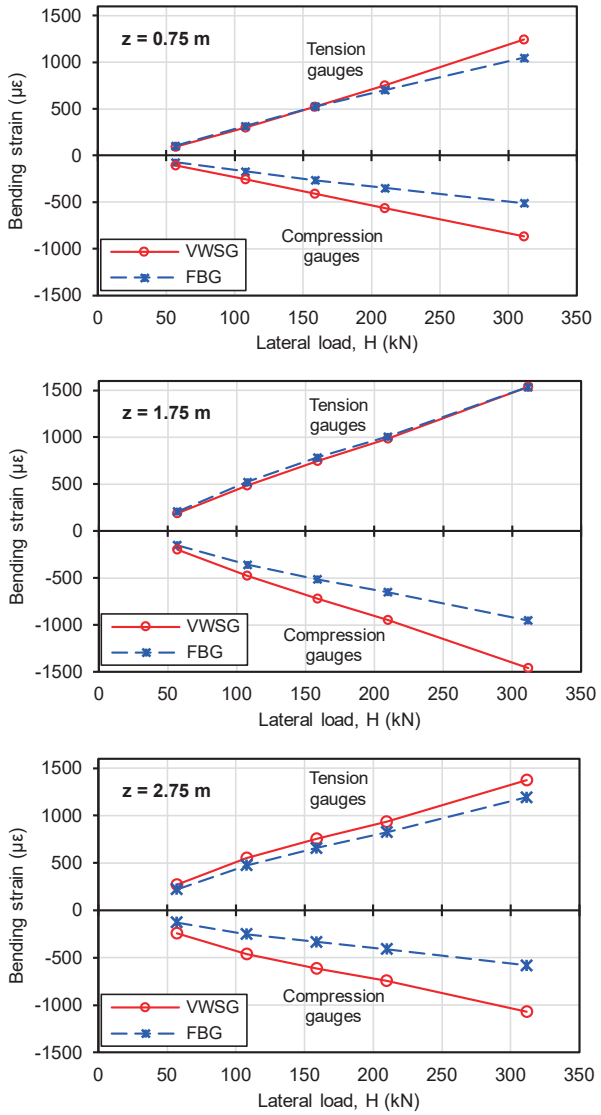

Fig. 5. Bending strains at various depths with monotonically increasing lateral load.

Strains determined using the two types of gauge typically deviated from one another as the load magnitude was increased. This was particularly evident in the compressive gauges. Tensile strain readings were in better agreement over a larger load range.

Percentage differences in compressive and tensile strain between the two gauge types were calculated using Equation 3, defined such that a positive difference indicates a larger VWSG reading.

$$\%\ \text{Strain difference} = \frac{\varepsilon_{VWSG} - \varepsilon_{FBG}}{\varepsilon_{VWSG}} \cdot 100\% \qquad (3)$$

The percentage differences in compressive strain and tensile strain at each depth as lateral load was monotonically increased are plotted in Fig 6.

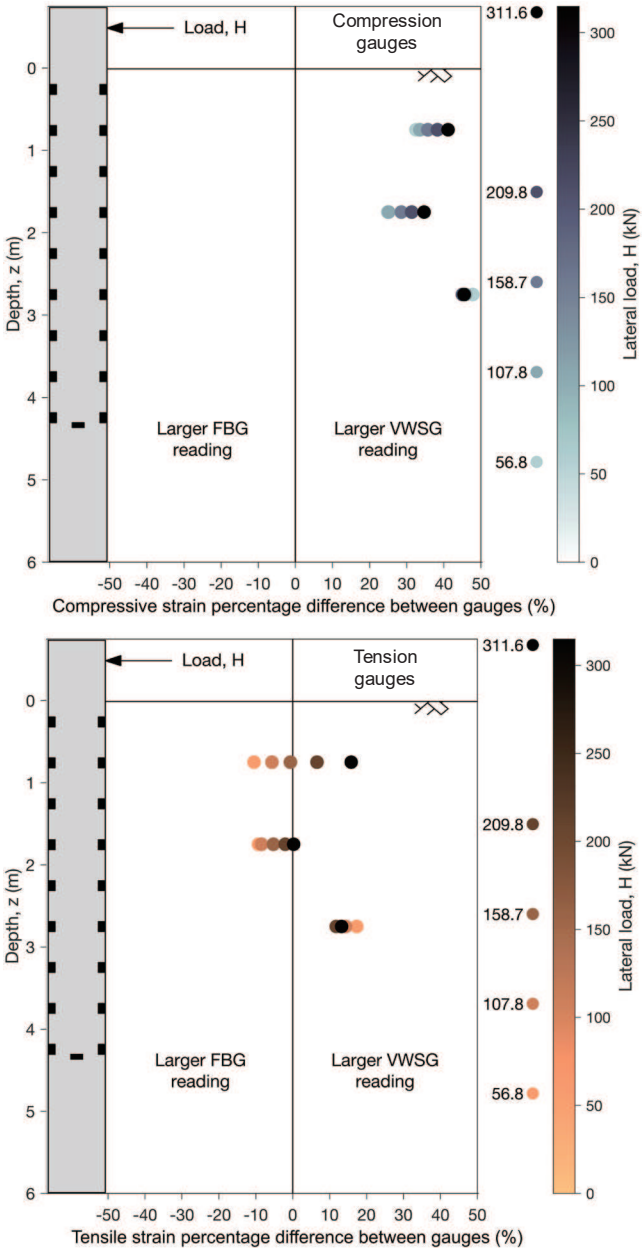

Fig. 6. Percentage difference in bending strains from different strain gauges under monotonically increasing lateral load.

© 2022 KOREAN GEOTECHNICAL SOCIETY (KGS), Seoul, Korea, ISBN 978-89-952197-7-5

Fig. 6 shows increasing percentage differences in compressive strain with increasing lateral load at z =0.75 m and z =1.75 m. At 2.75 m the difference was relatively constant, but of greater magnitude. The FBGs consistently underreported compressive strains. The tensile strains measured by the two gauge types were in better agreement, as seen in Fig. 6. The range of differences due to increasing load reduced with increasing depth.

The percentage difference between the bending moment determined from the FBGs (M_{FBG}) and the VWSGs (M_{VWSG}) is given by Equation 4.

$$\%\ \text{Moment difference} = \frac{M_{VWSG} - M_{FBG}}{M_{VWSG}} \cdot 100\% \qquad (4)$$

The percentage difference in bending moment with depth (z) as lateral load magnitude was increased in a monotonic load test is plotted in Fig. 7. These differences can be attributed to the differences in compressive and tensile bending strain.

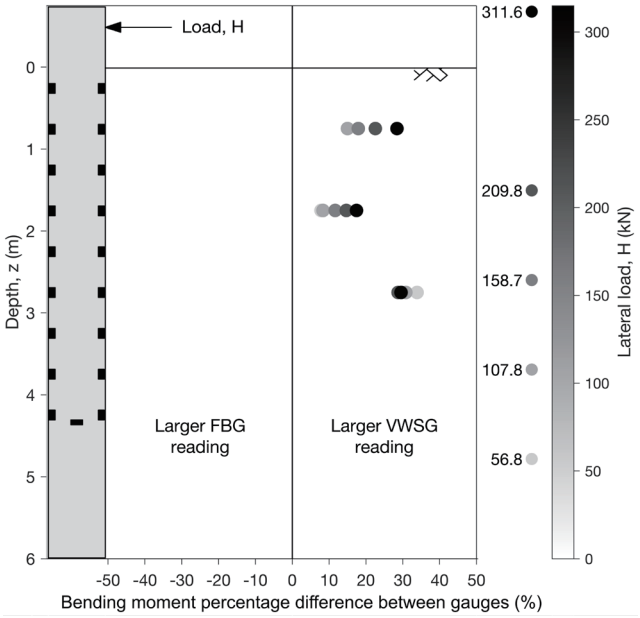

Fig. 7. Percentage difference in bending moments calculated using different strain gauges under monotonically increasing lateral load.

The bending moment variation between gauges increased with increasing lateral load at the shallow depths of 0.75 m and 1.75 m. A narrower range of differences is evident at 2.75 m. In the reported test, underpredicted FBG compressive strains were often compensated for by larger FBG tensile strains, reducing the percentage difference in the calculated bending moment, resulting in a maximum difference of around 30%. In the case where a prototype structure is being modelled or a numerical model is being calibrated through large-scale physical modelling, VWSGs may be the more reliable option to accurately quantify the magnitudes of bending strains and moments.

5 CONCLUSIONS

The following conclusions were drawn from this study:

- Closer FBG spacing than that of the VWSGs allowed greater detail of structural cracking to be captured.
- FBGs performed well in tension measurement. The FBGs and VWSGs recorded tensile strains within 20% of each other at all depths and load magnitudes.
- FBGs underreported compressive strain compared to the VWSGs. VWSG compressive strain readings were consistently in excess of 20% greater than the FBG readings.
- At shallower depths the percentage difference between gauge readings increased as lateral load magnitude increased. At greater depth, where bending moments and strains would be of lesser magnitude, variations between the gauges were larger and were constant with increasing load.
- Fibre optic sensing was suggested to be the more suitable option for structural health monitoring. VWSGs were deemed more suitable for large-scale physical modelling of a prototype structure.

ACKNOWLEDGEMENTS

The authors gratefully acknowledge the financial support of the UK Engineering and Physical Sciences Research Council (EPSRC) Global Challenges Fund under the WindAfrica project, Grant Ref: EP/P029434/1.

REFERENCES

da Silva Burke, T.S., Jacobsz, S.W., Elshafie, M.Z.E.B. & Osman A.S. 2022. Measurement of pile uplift forces due to soil heave in expansive clays. *Submitted for publication*.

BS EN 1992–1:2004. *Eurocode 2: Design of Concrete Structures*. London: British Standards Institution.

FBGS 2020. *Datasheet: Strain Measurements Wire SMW-01*. v15007_2. FBGS International NV.

Gaspar, T.A.V., Osman, A.S., Augarde, C.E., Coombs, W.M., Toll, D.G, Moghaddasi, H., Charlton, T.J., Jacobsz, S.W., Smit, G., da Silva Burke, T.S., Murison, R.A., Biscontin, G., Haigh, S.K., Al-Haj, K.M., Elshafie, M.Z.E.B., Elarabi, H., Elsharief, A.M., Zein, A.K.M, Abdelatif, A.M.O. & Rimoy, S.P. 2022. Investigating the design of piled foundations for wind turbines in swelling clays. *Proceedings: 20th International Conference on Soil Mechanics and Geotechnical Engineering, Sydney, Australia, 1–5 May 2022.* ISSMGE.

Geosense 2021. *Instruction Manual: Vibrating Wire Strain Gauges*. Version 1.8. Geosense Ltd.

Mosley, W.H., Hulse, R. & Bungey, J.H. 2012. *Reinforced concrete design to Eurocode 2*. London: MacMillan.

Murison, R.A., Jacobsz, S.W., da Silva Burke, T.S., Gaspar, T.A.V. & Osman, A.S. 2022. Comparison of swell behaviour of highly expansive clay through field monitoring and centrifuge modelling. *Proceedings: 20th International Conference on Soil Mechanics and Geotechnical Engineering, Sydney, Australia, 1–5 May 2022.* ISSMGE.